LOAD CONTROL OF A 300 h.p. TUNNELLING MACHINE: CONTROLLER MODIFICATION AND TESTING FOR UNDERGROUND TRIALS

by

J.B. Edwards and S.M. Sadreddini

Department of Control Engineering,
University of Sheffield,
Mappin Street, Sheffield S1 3JD.

Research Report No. 230

June 1983

N.C.B. Research Contract Ref. No. 226072

SUMMARY

Following the analysis and digital simulation described in Research Report No. 220[1] an analogue simulator of the tunnelling machine is described and the performance of the existing, real life load controller connected to the simulator is examined. Its performance is shown to accord closely with that predicted by pure simulation. The derivative-power, lead/lag compensator designed in R.R. 220 is implemented with additional passive components within the real controller and shown to produce the considerable improvements in stability and accuracy expected. The compensator is shown to behave equally well when load control is used in an overriding mode. Some circuit improvements are made to ease the tuning of the system's load limit.

1. INTRODUCTION

A description, dynamic analysis and digital simulation of the cutting operation of the 300 h.p. tunnelling machine, operating at Cadley Hill Colliery, were presented in Research Report No. 220, April 1983. The object of the research and development described in this continuing series of reports in the elimination of gearbox failures associated with the arduous and fluctuating loads encountered by the rock cutting head of this machine.

Since the writing of the previous report, the digital simulation has been successfully transferred to two analogue computers to permit the inclusion of a load control amplifier unit, (identical to that currently in use on the machine), for real time investigation and to permit the controller changes recommended in research report 220 to be implemented and tested. As shown in later sections of the present report, this operation has been successfully completed and demonstrated to members of the M.R.D.E. Tunnelling Branch and associated technical services. One outcome of this demonstration and subsequent discussion was the recommendation that manual control of cutting speed should be constantly provided but subject to a load-control limit. This was indeed the objective of the existing system that was not fully realised due to stability problems and certain electronic difficulties in combining the speed- and load-control systems. By incorporating the derivative power feedback and an additional lag circuit, specified in research report 220, the stability problem has now been solved (accepting the adequacy of the mechanical system simulation) and further modifications to the summation circuitry for the load and rate(speed) signals have allowed the maximum load limit now, (a) to be more precisely set and (b) to operate more accurately.

The present report describes the circuit modifications involved and compares the performance of the existing control amplifier before and after modification.

2. ANALOGUE SIMULATION

It will be recalled that the system was described in Research Report 220 by the following equations:

$$dy/dt = v(t) - v(t-T) \quad (1)$$

$$P_m = k_h\, y \quad (2)$$

$$P_i = k_2\, P_m/(1 + T_m D) \quad (3)$$

where

y = bite/cutting pick

v = annular velocity of the cutting head

P_m = mechanical power consumption of the cutting head

P_i = electrical power consumption of the 300 h.p. induction motor driving the head

$D = d/dt$

T = time interval between successive pick arrivals in any one plane (taken to be 1.8s)

k_h = rock hardness, pick sharpness factor nominally = 3200 kw/m

k_2 = 1/average motor and drive efficiency = 1.25

T_m = inertial time constant of motor and drive (taken initially to be 0.5s but subsequently calculated to be 0.048s)

The unmodified continuous load control system assumed in Research Report 220 was modelled thus

$$v = v_r/(1 + T_h D) \quad (4)$$

$$v_r = k_1\, P_e \quad (5)$$

where

$$P_e = P_r - P_i' \quad (6)$$

and $$P_i' = P_i/(1 + T_f D) \quad (7)$$

where

v_r = demanded annular speed

P_e = load error signal (in kW)

P_i' = filtered measurement of P_i (in kw)

and P_r = preset reference power consumption (in kw)

k_1 = adjustable controller gain (or sensitivity)

T_h = time constant of the electrohydraulic servo (assumed to be 0.25s)

and T_f = time constant of the power transducer filter (so far assumed to be negligible)

Proposed modifications to the simple proportional control algorithm involved the replacement of control equation (5) by

$$v_r = k_1(P_e' - P_d) \tag{8}$$

where

$$P_e' = P_e/(1 + T_L D) \tag{9}$$

and $$P_d = P_i' k_d T_d/(1 + T_d D) \tag{10}$$

where

P_d = added derivative power feedback signal

P_e' = power error signal after an added lag filter

T_L = time constant of the added lag

T_d = time constant of the derivative feedback network

and k_d = derivative gain of the system

Fig. 1 shows the analogue circuit diagram incorporating both forms of control (i.e. eqns. 5 and 8) carefully scaled to avoid amplifier saturation at the expected signal levels. Two VIDAC 680 computers, 1 and 2, are used, the amplifiers and potentiometers of computer 2 being distinguished by asterisks (*) in Fig. 1. The diagram also shows the circuit changes involved in substituting the real controller (from the actual tunnelling machine) for the computer-implemented control laws. A fourth-order Pade approximation circuit, involving integrators $A1^*$, $A2^*$, $A3^*$, $A4^*$ is used to simulate the time-delay, T, between cutting pick arrivals. Amplifier M2B returns the simulated rate-feedback signal (measuring v(t)) to the control amplifier via trunk 11 whilst amplifiers M1B and B4 return the direct and inverted forms of the simulated power

feedback signal via trunks 6 and 13 respectively. The output of the control amplifier, (loaded with a dummy 800Ω resistor simulating the electrohydraulic servo valve motor) is returned to the VIDAC simulator via trunk 16 and amplifier M2A as shown. Recordings of annular speed v(t) and input power $P_i(t)$ are made via trunks 5 and 4, from amplifier A1 and B5 respectively.

As the results in Section 3.1 clearly demonstrate, the analogue simulation produced results virtually identical to those produced digitally and included in Research Report 220. This agreement was achieved despite the approximation inevitably introduced by the fourthorder Pade circuit: This is because the overall system oscillates at a frequency of around 1/2T Hertz and the phase error if the circuit at 1/T Hertz is known to be only 1^{o}.

Having established this agreement between the digital and analogue prediction, it was possible to proceed with confidence to the connection of the real life controller to the analogue simulator.

3. RESULTS

3.1 With Computer Simulated Controller

Fig. 2 shows the analogue response at start-up and to a 50% step increase in rock-hardness using the following parameters

$k_1 = 0.0003$, $k_2 = 1.25$	$T_d = 0.1s$
$k_h = 3200 \rightarrow 4800$ kw/m bite	$T_m = 0.5s$
$k_d = 2.69$	$T_h = 0.25s$
$T_L = 0.75s$	$P_r = 200$ kw

i.e. for the system using the derivative power compensator designed in Research Report 220. The recording clearly agrees very closely with the digital simulation response shown in Fig. 7 of that report, in respect of transient amplitudes, frequencies and steady state errors.

To ensure that the new compensater was not disguising errors in the plant simulation, the trace of Fig. 3 was also produced for the same parameter settings but with the new compensator omitted (i.e. with k_d and T_f set to zero). The response is clearly in very close accordance with that for the same system (Fig. 5) in Research Report 220. The predicted benefits of the new compensator are again obvious.

3.2 Using the Real Control Amplifier (Unmodified)

Using the following transducer parameters (supplied by M.R.D.E.) viz:

power transducer gain = 1 Volt per 200 kw

rate transducer output ≃ 6 volt for maximum swash angle (≡ 7/8" of potentiometer travel)

it was possible to scale the output signals from the VIDAC I computer to produce nearly identical inputs (for given operating conditions of speed and power) to those received by the control amplifier under real life conditions. This scaling was accomplished by potentiometers B2 and A2 respectively in Fig. 1. For example, when amplifier A3 produces 8 volts (i.e. 0.8 machine units) corresponding to P_i = 200 kw, amplifier M1B and B4 return signals of 8 x 0.125 = 1 volt, as required to the control amplifier, potentiometer B2 being preset at 0.125.

As regards scaling of the control valve signal passing from the control amplifier to 'hydraulic integrator' A1, this operation was accomplished by setting potentiometer A1 to unity and adjusting the hydraulic loop 'gain' control in the control amplifier to produce the estimated hydraulic lag T_h = 0.25s. This gain control, along with the arrangement of the other adjustable amplifier controls is illustrated schematically in Fig. 4.

Figs. 5 to 7 show the performance of the existing (unmodified) control amplifier operating as a continuous, rather than an overriding

controller by leaving diode D1 (Fig. 4) out of circuit and by shorting the normally-closed control of the load/rate changeover relay as indicated so as to include both rate and load control simultaneously i.e. as in present practice. The percentage of load to rate control was reduced progressively through Figs. 5 to 7 to improve the stability of the unmodified system. The tests were made by varying the hardness factor k_1 from the nominal 3200 kw/m bite in increments of minus and plus 50% and the progressive reduction of oscillation achieved is obvious. It is also clear however, that the stability of Fig. 7 is achieved at the expense of accuracy, the load changing between limits of 70 and 126kw about a nominal condition of 107kw thus confirming earlier predictions based on pure simulation. The parameters used for obtaining Figs. 5 to 7 were

Load = 50%, 40%,20%

Rate = 20%, 27%,27%

Current feedback = 40%

Hydraulic loop 'gain' = 10%

3.3 With the Compensator Added to the Real Control Amplifier

Circuit modifications indicated in Fig. 8 were effected to implement, as closely as possible, the lead/lag, derivative power compensator derived in Research Report 220. The lag capacitor C_L was calculated as follows:

Derived lag T_L = 0.75s (see Research Report 220)

$\therefore$ $C_L R_{13}$ = 0.75s , R_{13} = 10 KΩ

$\therefore$ C_L = $0.75. \ 10^6/10^4$ = 75 μF.

C_L was therefore set at 69 μF, this being the nearest convenient value.

Because of signals sign problems, and to avoid the need for an additional inverting amplifier, the derivative action was entered via the

rate amplifier IC - 2 rather than directly into OA2. This, of course, suffers the disadvantage of introducing some interaction of the rate and derivative feedback controls during system tuning so making this task rather more tedious than it need be and, in a final implemenation, a separate derivative amplifier should be included. A consideration of Fig. 8 reveals that the effective transfer-function $G_d(D)$ of the derivative path, as implemented, is

$$G_d(D) = \frac{(\text{RV8 setting})\ R_{17} C_d D}{(\text{RVC})(\text{RVA})(1 + R_d C_d D)} * (\text{Derivative pot. setting}) \qquad (11)$$

clearly indicating the interaction of the settings of the load (RVA) - rate (RV8) - and current feedback (RVC) - potentiometer settings. These are operated typically at values of 50, 40 and 27% respectively and R_{17} is 10 kΩ so that, selecting values of R_d and C_d = 2 kΩ and 30 μF respectively, yields the numerical transfer function

$$G_d(D) = \frac{0.27\ 10^{4}\ 30\ 10^{-6}\ D}{0.4\ 0.5\ (1 + 2\ 10^{3}\ 30\ 10^{-6} D} = \frac{0.405\ D}{1 + 0.06D} \qquad (12)$$

at 100% setting of the derivative potentiometer, compared to the designed transfer function (see Research Report 220) of

$$G_d(D) = \frac{k_d T_d D}{1+T_d D} = \frac{2.69\ 0.1\ D}{(1 + 0.1D)} = \frac{0.269\ D}{1+0.1\ D} \qquad (13)$$

The network thus allows an effective value for k_d to be achieved of up to 50% greater than the theoretical value estimated to be necessary in Research Report 220. (The somewhat lower value of T_d actually implemented should improve the system phase margin slightly).

Figs. 9 and 10 show the responses rock to hardness changes of ± 50% obtained on inclusion of the derivative compensator with the following potentiometer settings:

Load	Current Feedback	Rate	Hydraulic loop Gain	Derivative	Fig.
50%	40%	27%	10%	50%	9
60%	40%	27%	10%	80%	10

Comparison with the uncompensated system of Fig. 7 shows that, as expected, the load errors are now much improved (for similar degrees of stability) through being able to operate now at higher load gains. The 50% hardness change now produces load changes from 90 to 120kw (Fig. 10) about an average of 110 kw compared to 70 to 126 kw (Fig. 7) previously, about an average of only 107 kw. The results verify the effectiveness of the compensation when implemented practically on the real controller.

4. IMPLEMENTATION OF OVERRIDING LOAD-CONTROL

Experience with the tunnelling machine at Cadley Hill Colliery has revealed that load-control is better when used in an overriding mode rather than continuously. Speed- or so-called Rate-control is thus available to the machine driver over the full-speed range up to the point at which the preset load reference signal P_r is exceeded, whereupon the rate control is overridden until such time as the load returns to less than the reference value. (With continuous load control scheme used previously, rate control was available as a switched option to the operator, but with the rate-reference v_r limited to a very low value intended only for inching the cutting head into the material at the start of cutting operations).

The changeover from the earlier scheme to the present override system involved

(a) the bridging of the normally-closed changeover relay contact in Figs. 4 and 8 in an attempt to combine the rate and load control in amplifier OA2

(b) the insertion of the feedback diode D1 around the power error amplifier ½ IC1

and (c) reducing R 14 from 100 kΩ to 10 kΩ so increasing v_r significantly.

The same changeover was implemented in the laboratory at Sheffield but, when simulation trials of the overriding system were begun it was found that the changeover point was highly indistinct and highly dependant on the settings of the load and rate proportioning potentiometers RVA and RV8. A cleaner method of signal addition was therefore implemented by entering the rate error separately to amplifier OA2 via an independent input resistor R13 already available but previously unused.

Having implemented these changes, trials showed that changeover was now more distinct and independent of pot settings other than that of the load reference potentiometer RVF: as desired. Typical results are shown in Fig. 11 and 12, for the uncompensated system, and Fig. 13 for the compensated system, the latter two cases being tuned for adequate stability. The parameter settings are

Load	Current Feedback	Rate	Hydraulic loop gain	Derivative	Fig.
40%	40%	27%	10%	zero	11
20%	40%	27%	10%	zero	12
50%	40%	27%	10%	70	13

The load reference P_r was set to operate fractionally below the load required at a preset rate reference v_r in rock of nominal hardness (i.e. $\equiv$ 3200 kw/m). Load control is therefore effective following the + 50% hardness increase but is relatively ineffective when k_h falls to 1600kw/m. It is clear from Fig. 11 that the load change in the harder material is 10%, (146kw to 160kw) with excessive oscillation when using the uncompensated system. This error clearly increases to 21% (120 to 145kw) when stability is restored without resort to the new compensator as Fig. 12 shows. Use of the compensator (Fig. 13) clearly allows adequate stability with a load error of only 7.9% (155 to 167 kw). The advantages of using the compensator are therefore retained in the transfer from continuous to overriding load control.

5. CONCLUSIONS

An analogue simulator derived from the analysis of Research Report 220 has been set up that allows tests to be made on the dynamic performance of the real life load control amplifier for the 300 h.p. tunnelling machine. It has been shown to generate responses that are in close accord with those obtained purely by digital simulation in Research Report 220.

The derivative power lead/lag compensator designed in functional terms in Research Report 220 has been implemented by means of a few additional passive components (resistors,potentiometers and capacitors) connected into the spare amplifier provided by M.R.D.E. for these tests. The added networks have been shown to be quite as effective as pure simulation predicted, producing considerably more stable performance than the original system with only small static errors in the operating load despite large changes in simulated rock-hardness.

The system has been successfully converted to the preferred overriding type of load control so giving the operator full-range speed control within the preset load limit. To achieve a more distinct and easily set changeover, some modification to the addition of the rate and load error signals has been necessary.

All the necessary circuit changes are indicated in Figs. 4 and 8 which should be read in conjunction with M.R.D.E. drawing MRDSK-15392. The addition of extra amplifiers has been avoided in this implementation of the derivative-power compensator at the expense of some interaction in system tuning. Tuning would therefore be best accomplsihed on a surface power pack linked into the simulation to avoid time wasting during the commissioning of the system underground. Ideally, and in the longer term, an additional derivative power amplifier should be incorporated.

6. REFERENCES

(1) Edwards, J.B. 'Load control of a 300 h.p. tunnelling machine', University of Sheffield, Department of Control Engineering, Research Report No. 220. April 1983, 23 pp.

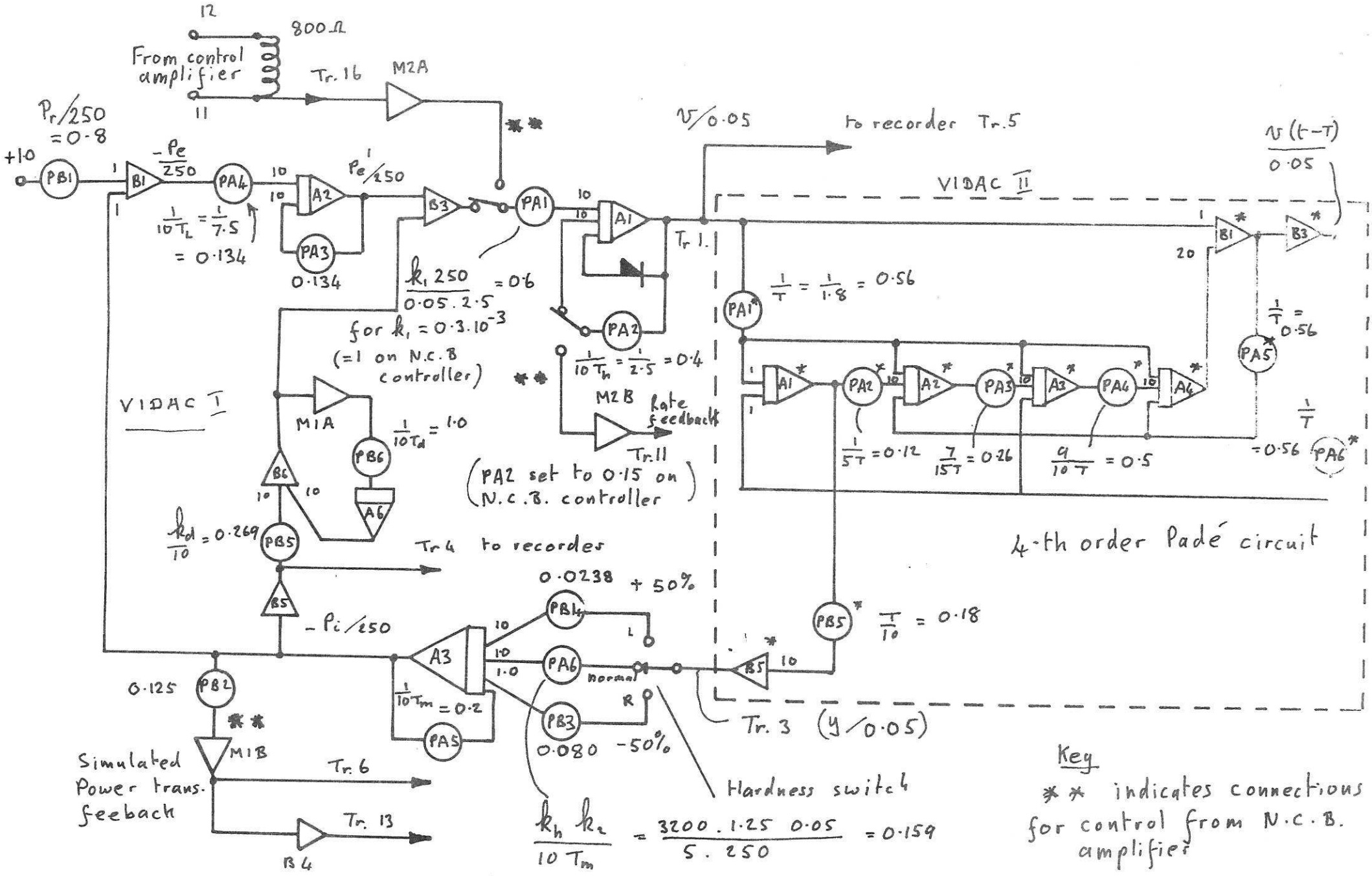

Fig. 1. Analogue computer diagram for machine simulation

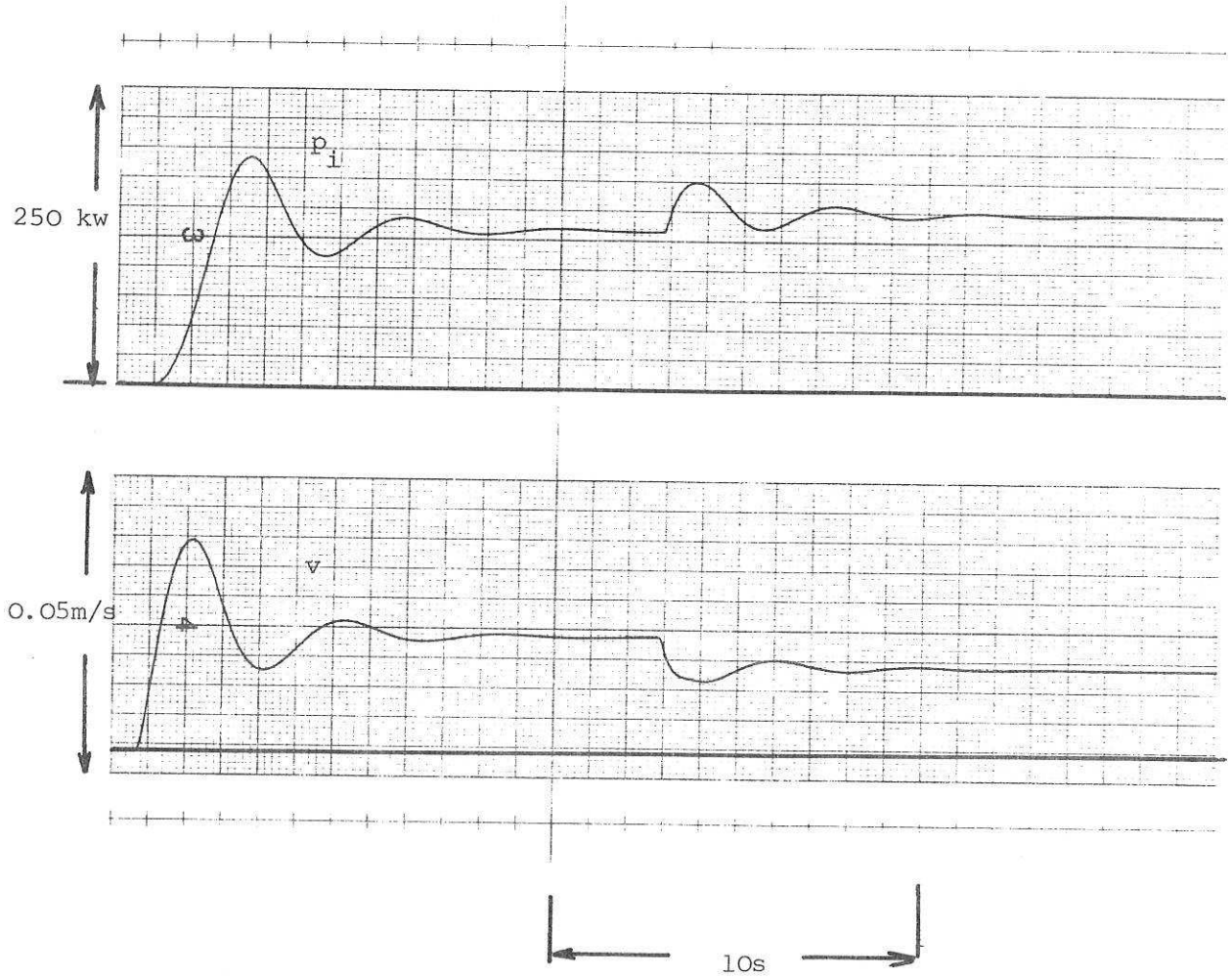

Fig. 2 Analogue simulation, with compensator. Response to switch-on and 50% increase in rock hardness.

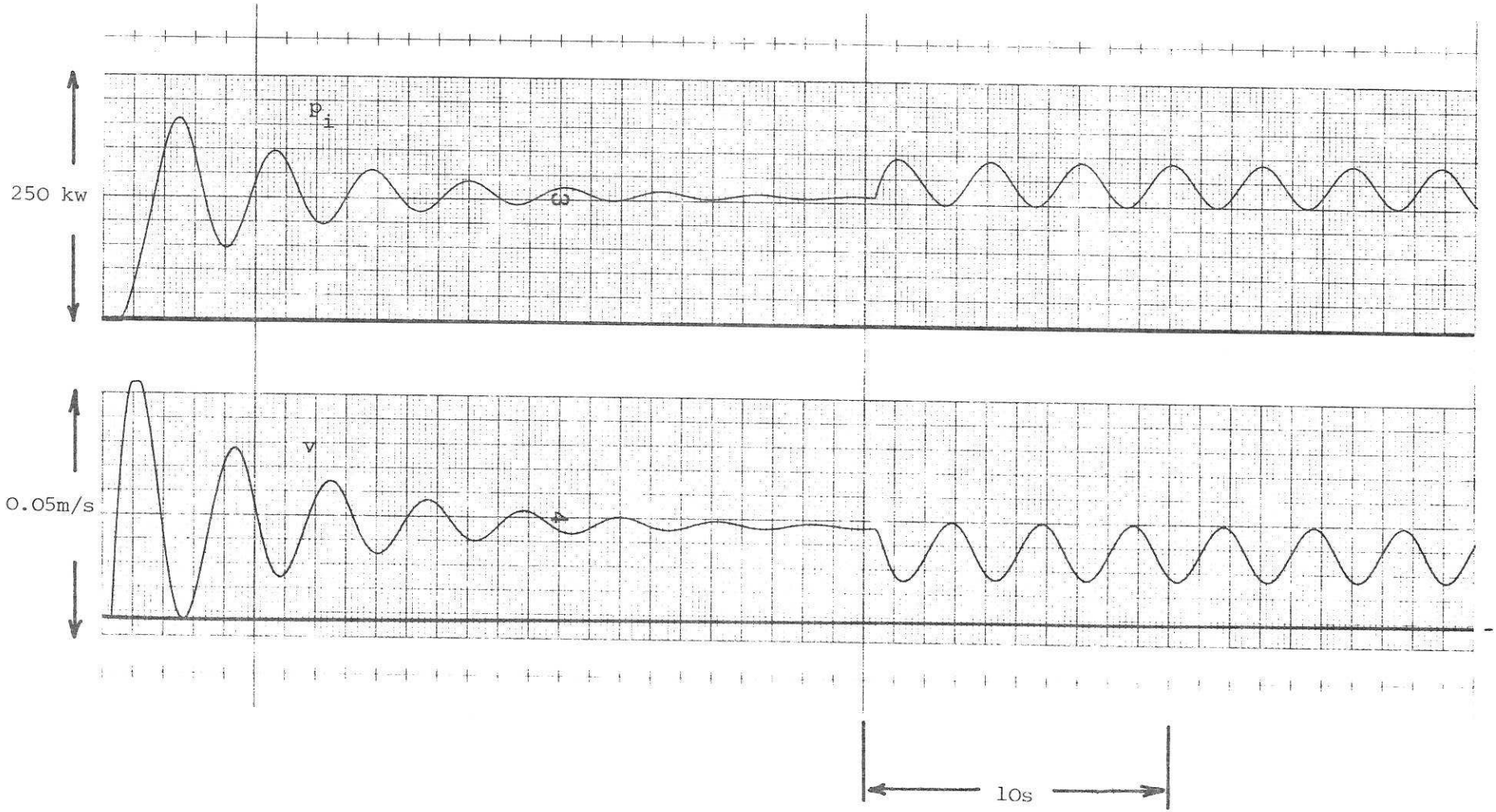

Fig. 3 Analogue simulation, without compensator. Response to switch-on and 50% increase in rock hardness

Fig. 4 Schematic of existing N.C.B. control amplifier (from MRSK 15392) before modification

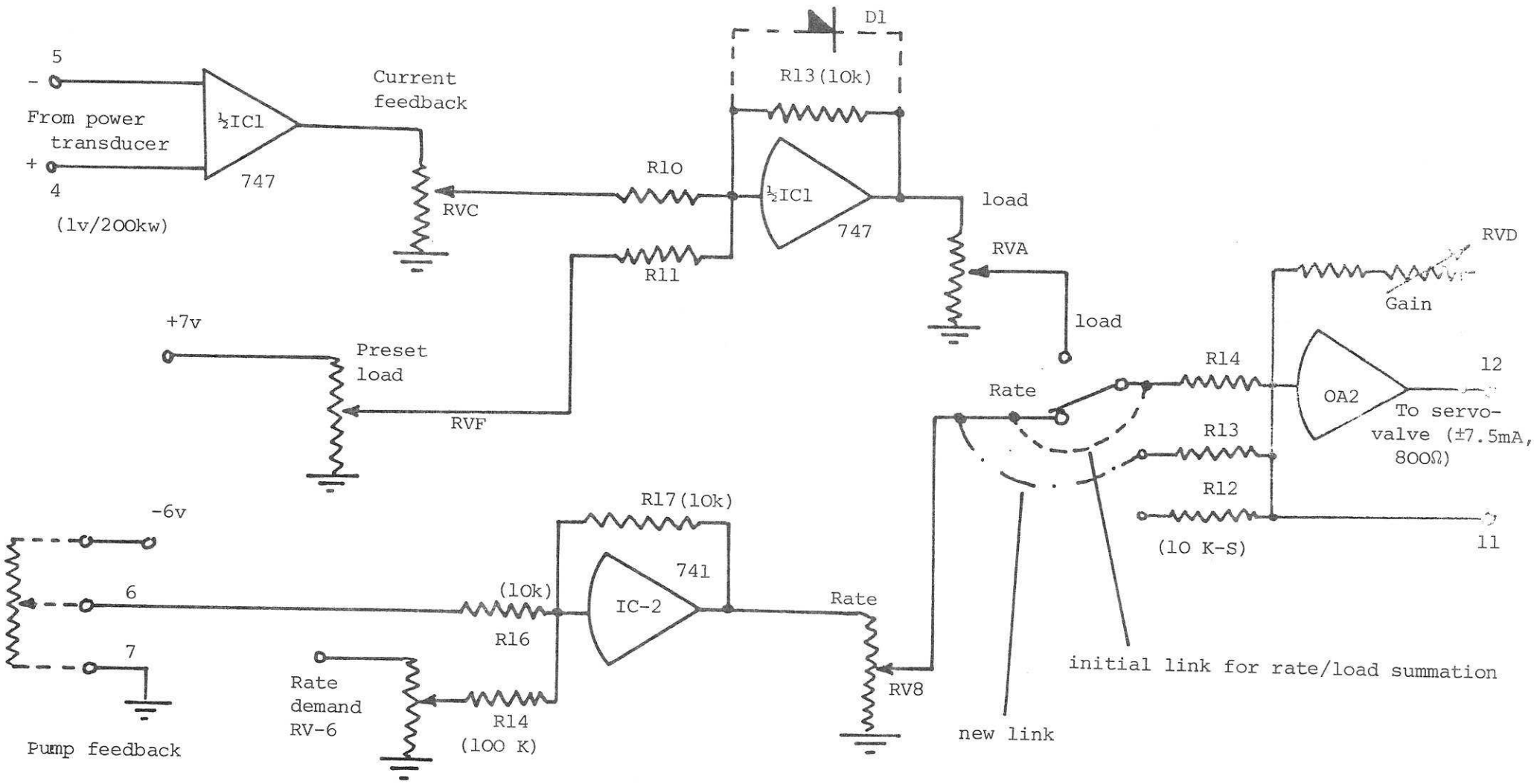

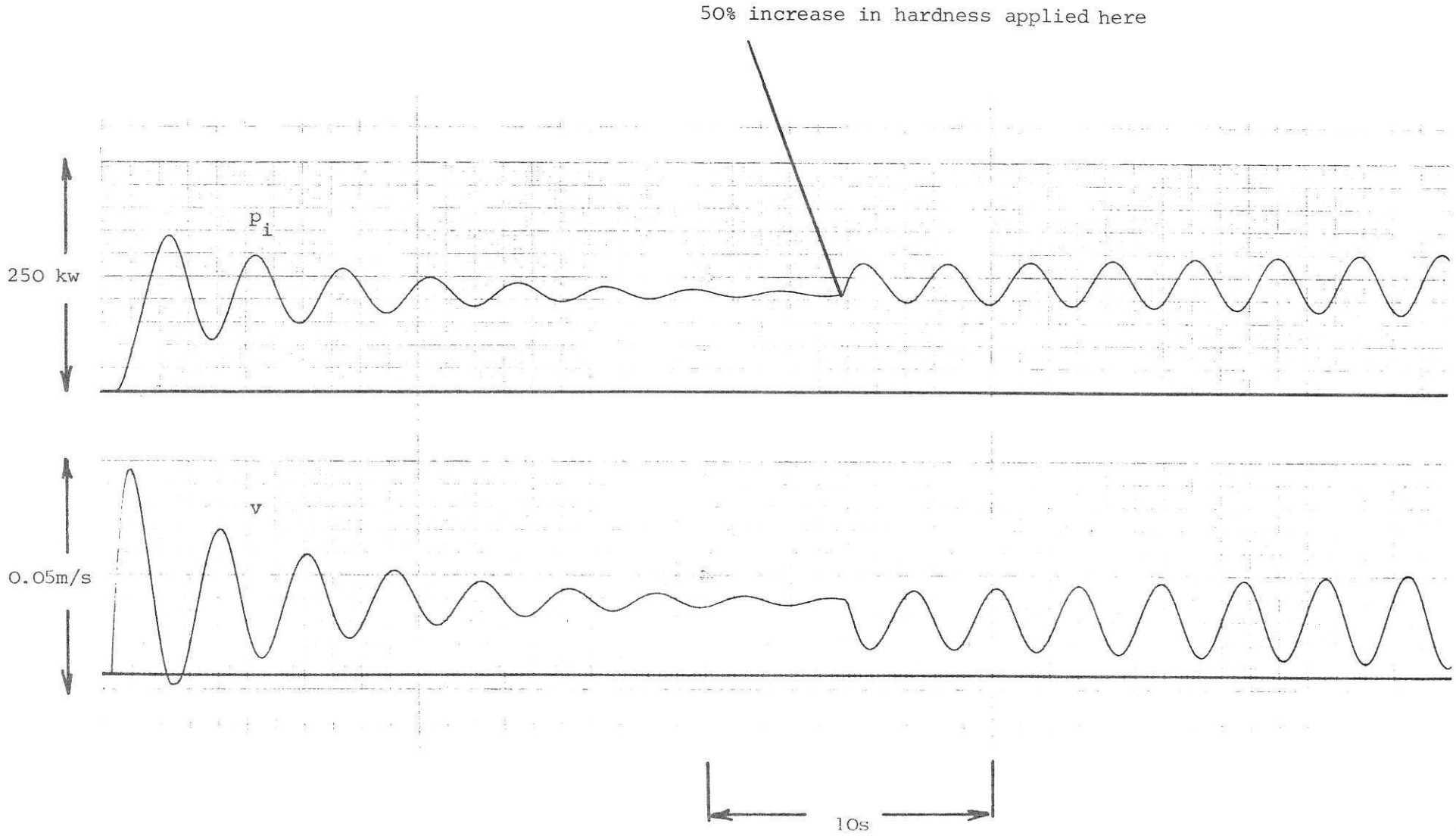

Fig. 5 Response of N.C.B. controller, unmodified. Load gain setting = 50%

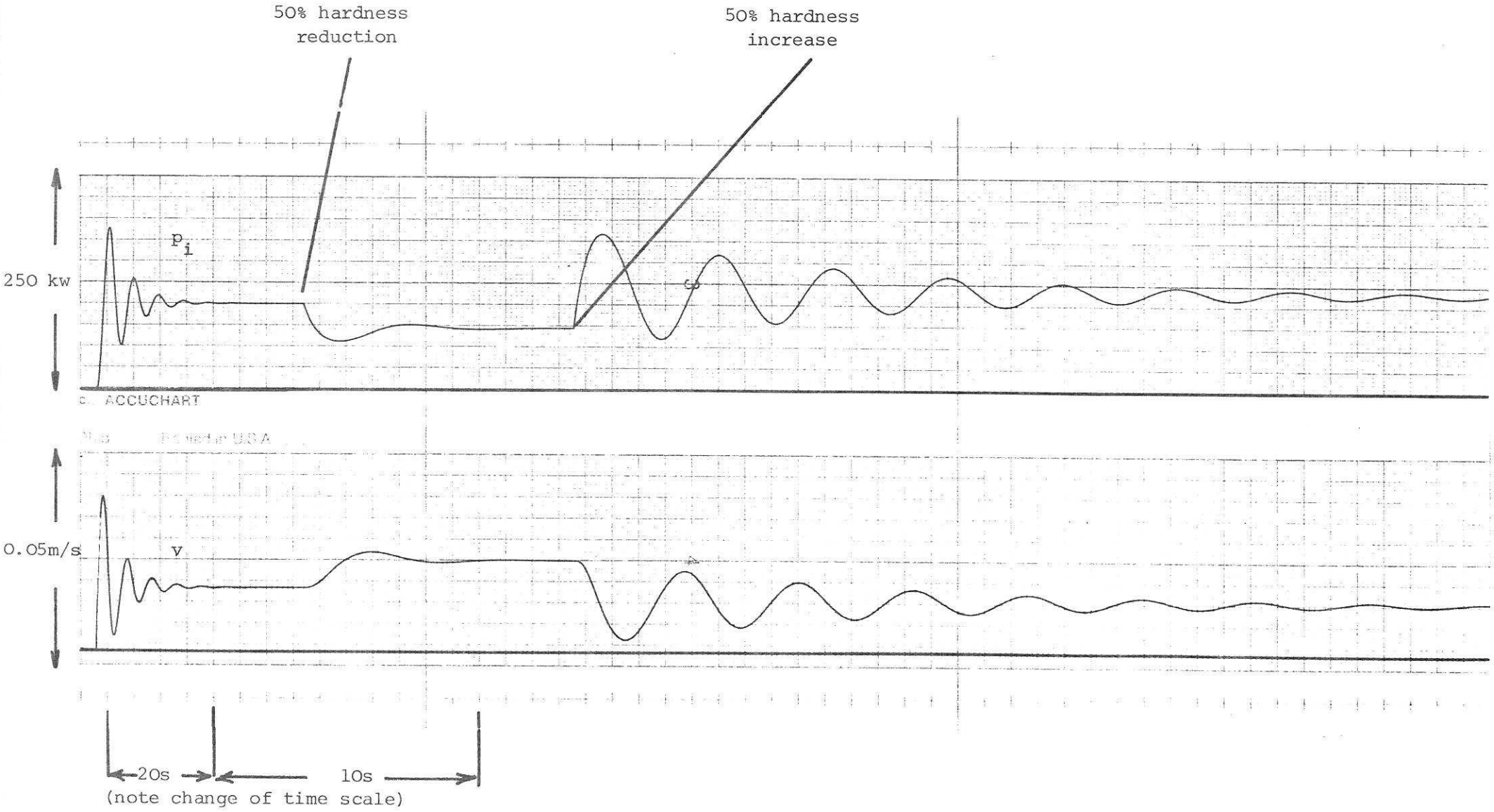

Fig. 6 Response of N.C.B. controller, unmodified. Load gain setting 40%

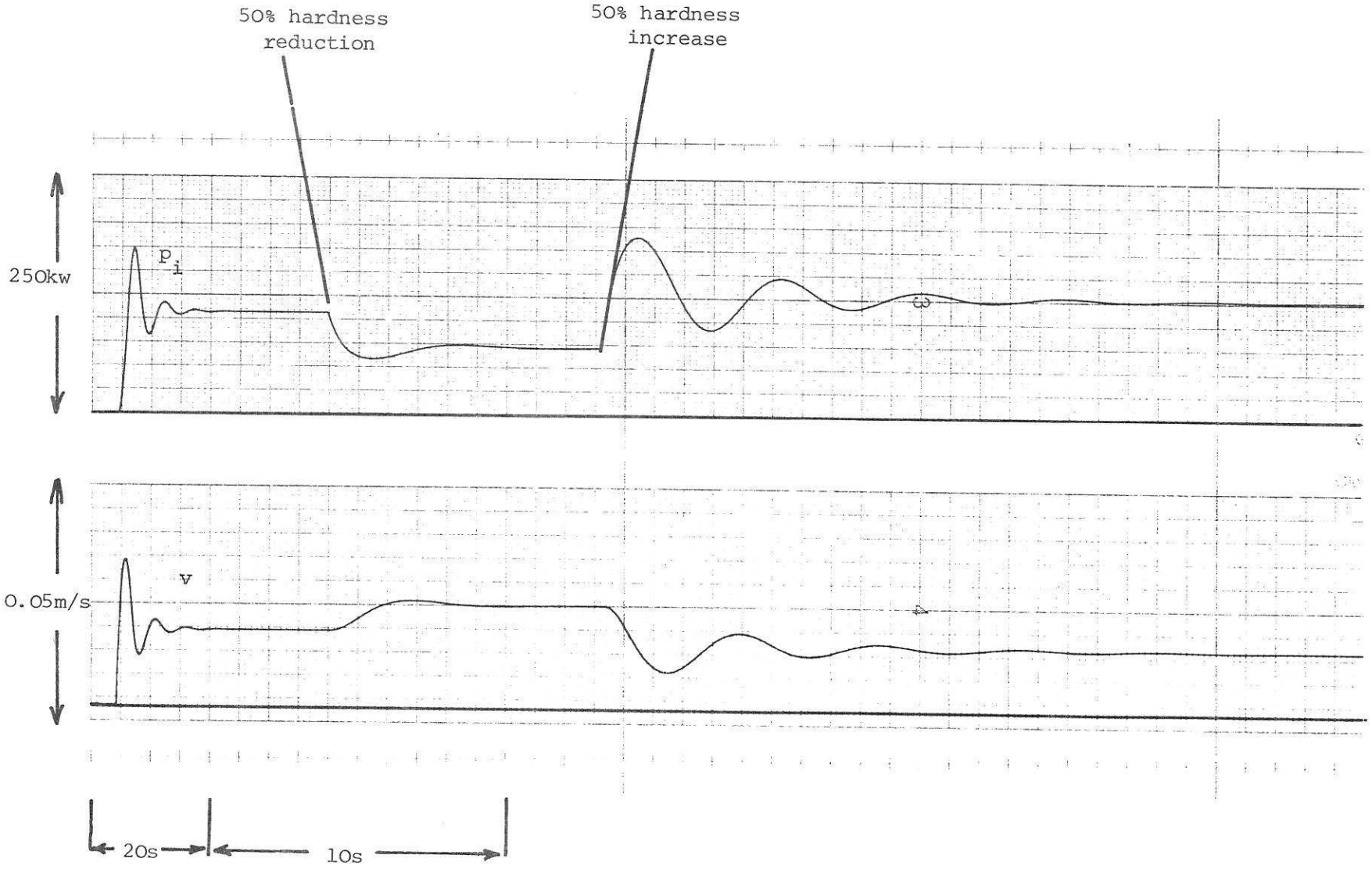

Fig. 7 Response of N.C.B. controller, unmodified. Load gain setting 20%

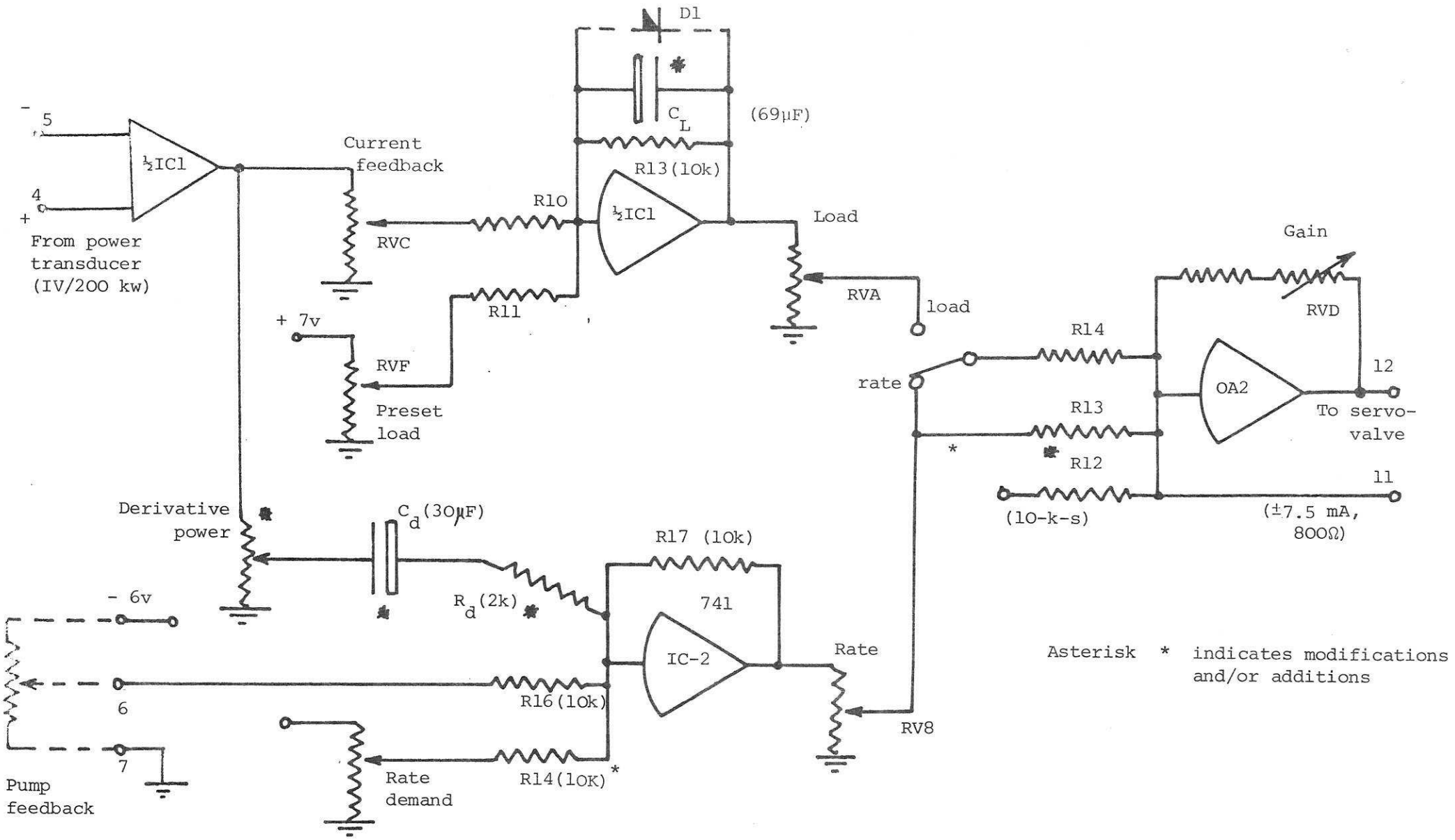

Fig. 8 Modifications to N.C.B. control amplfier (from MRDSK 15392) to implement compensator

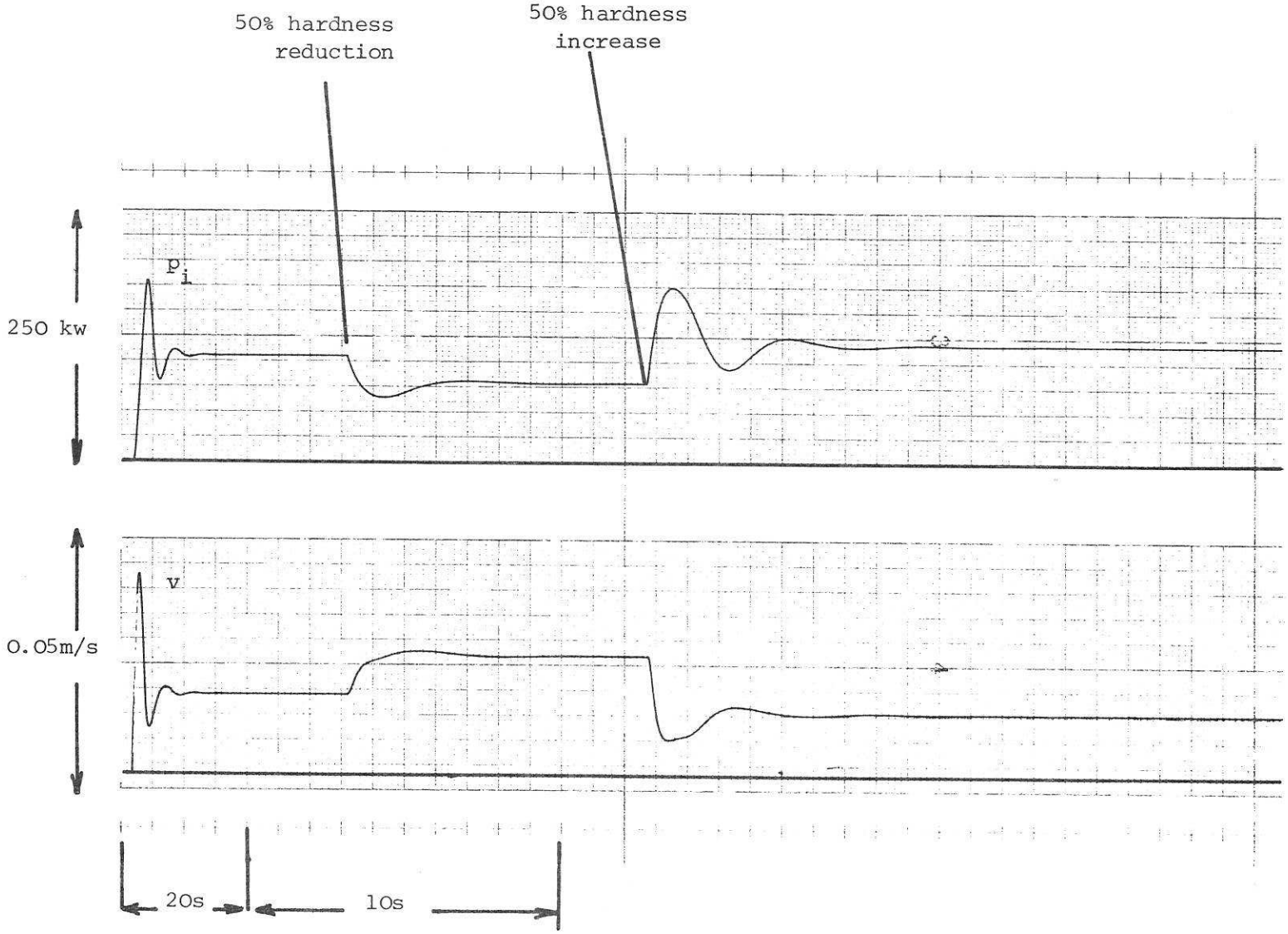

Fig. 9 Response of N.C.B. controller with compensator added.

Load gain setting = 50%, derivative gain setting = 50%

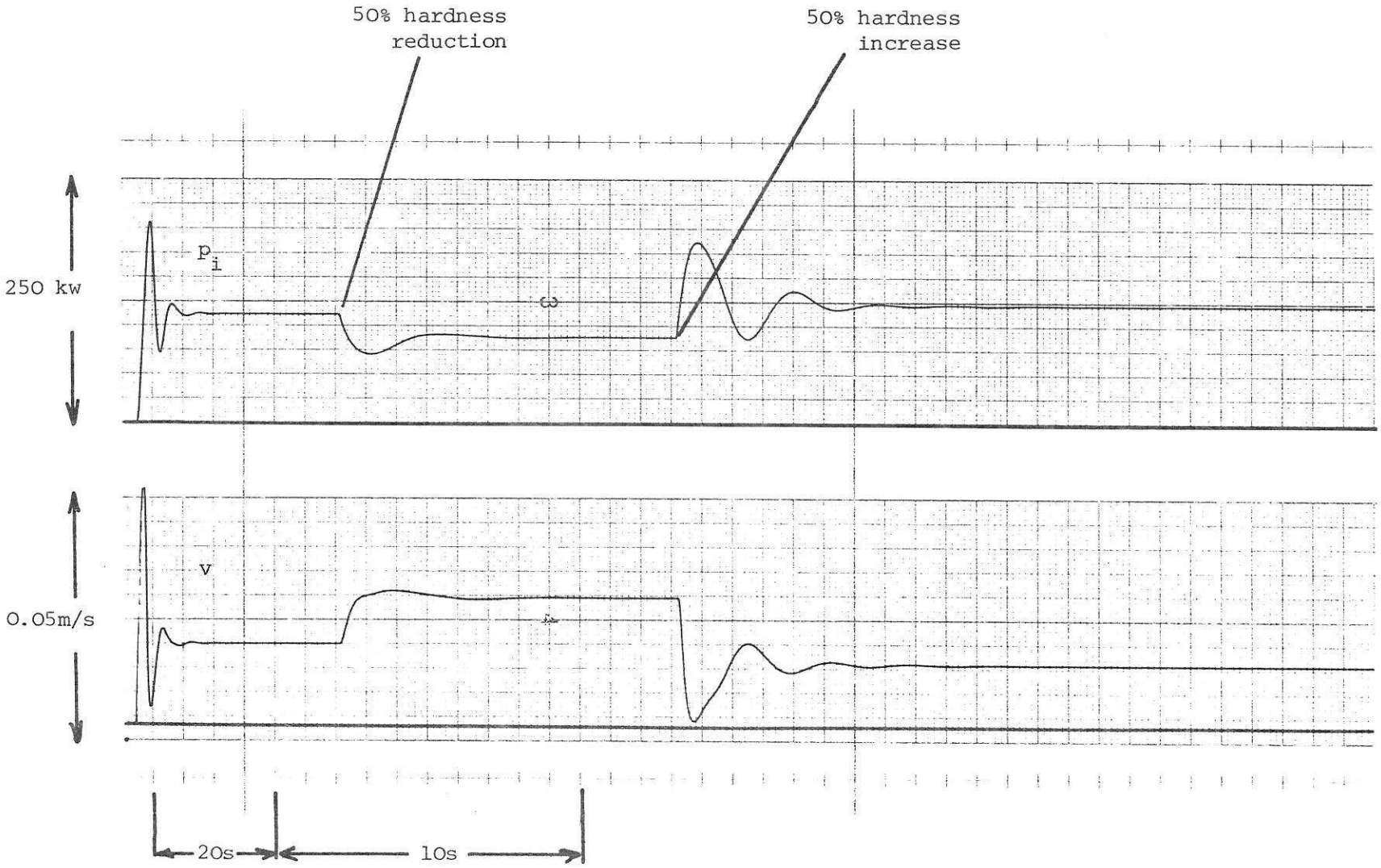

Fig. 10 Response of N.C.B. controller with compensator added load gain setting = 60%

derivative gain setting = 80%

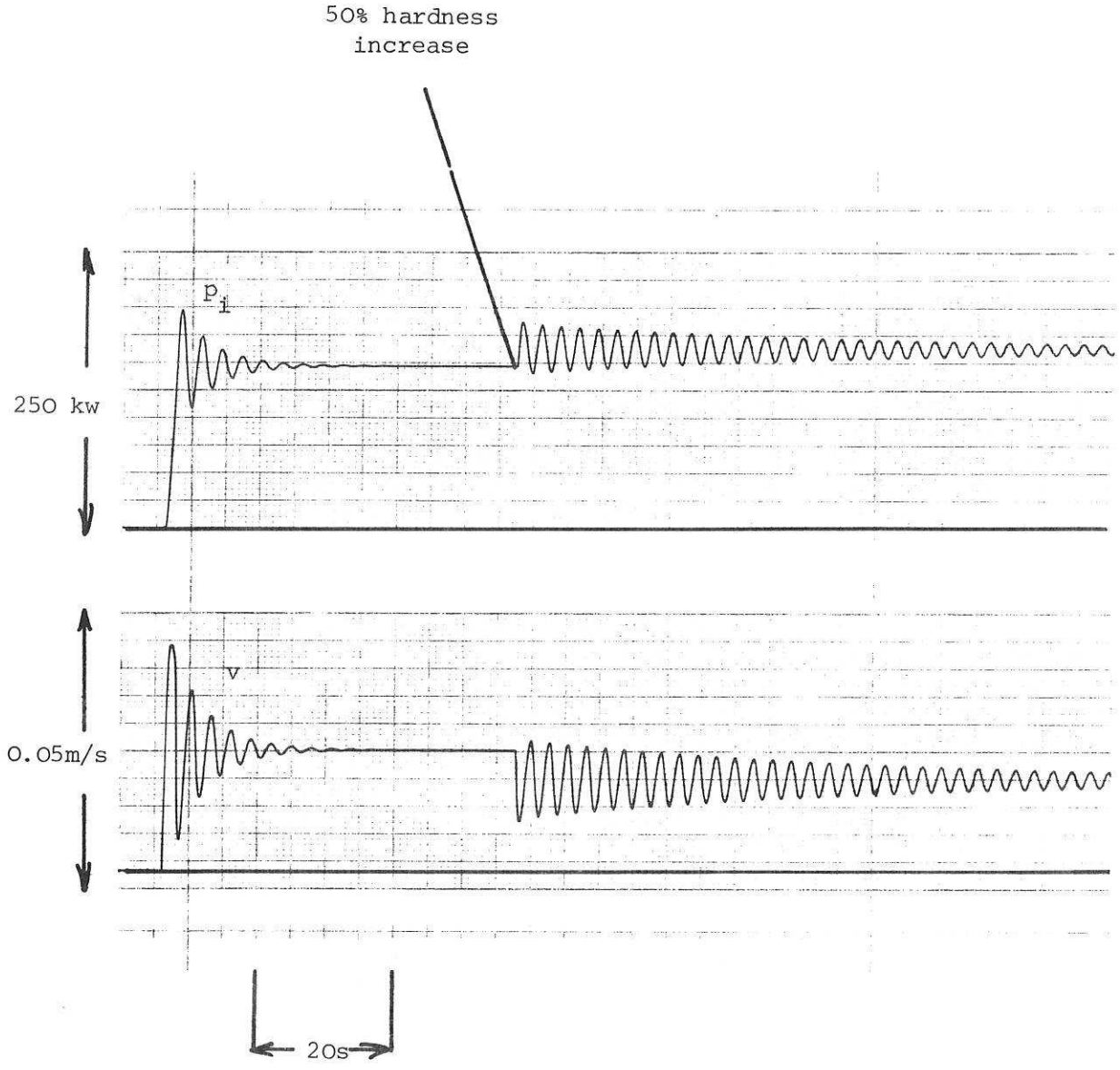

Fig. 11 Response of N.C.B. controller (unmodified) operating as an overriding load control (Load gain setting = 40%)

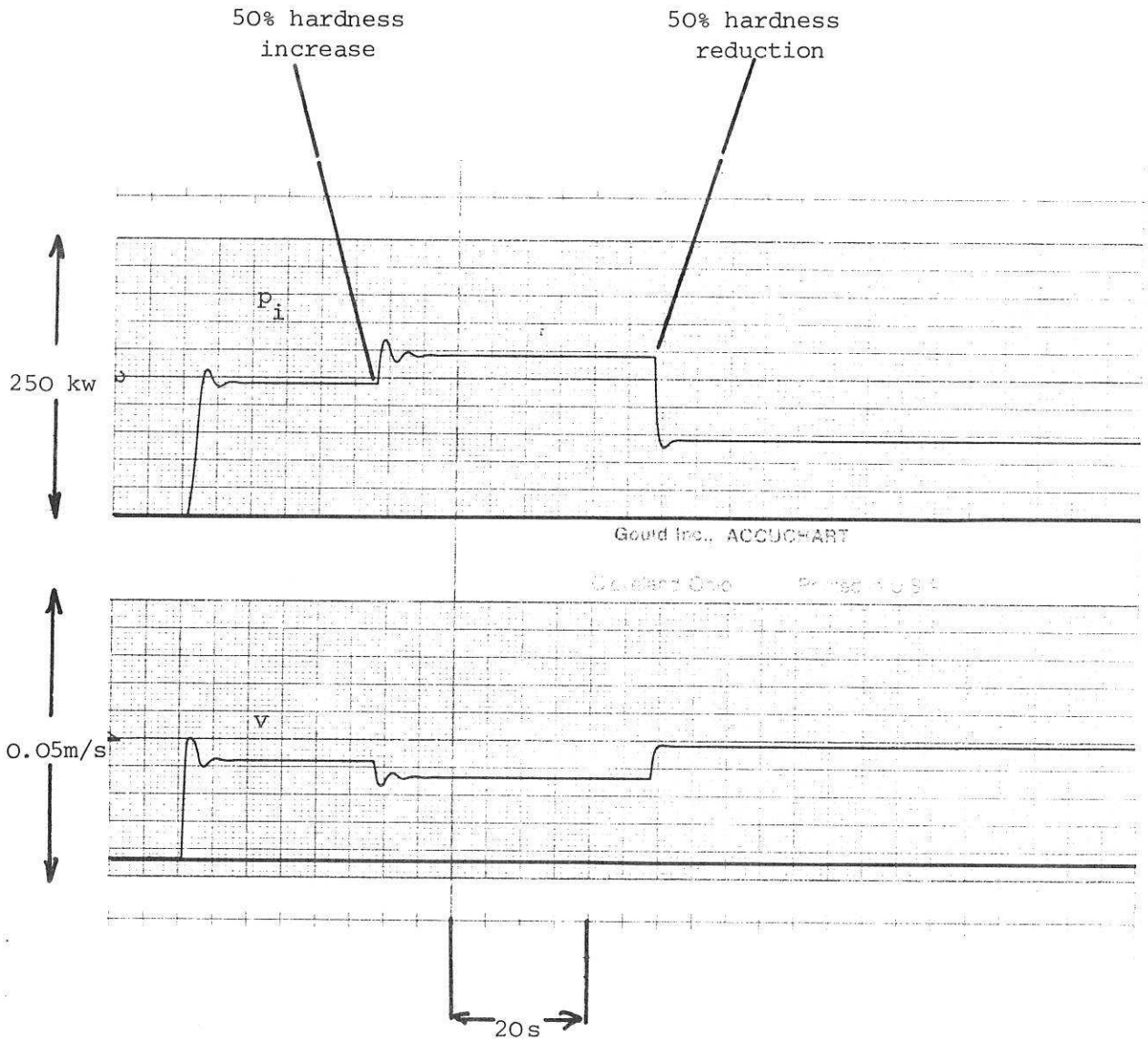

Fig. 12 N.C.B. controller in overriding mode (unmodified). Load gain setting = 20%

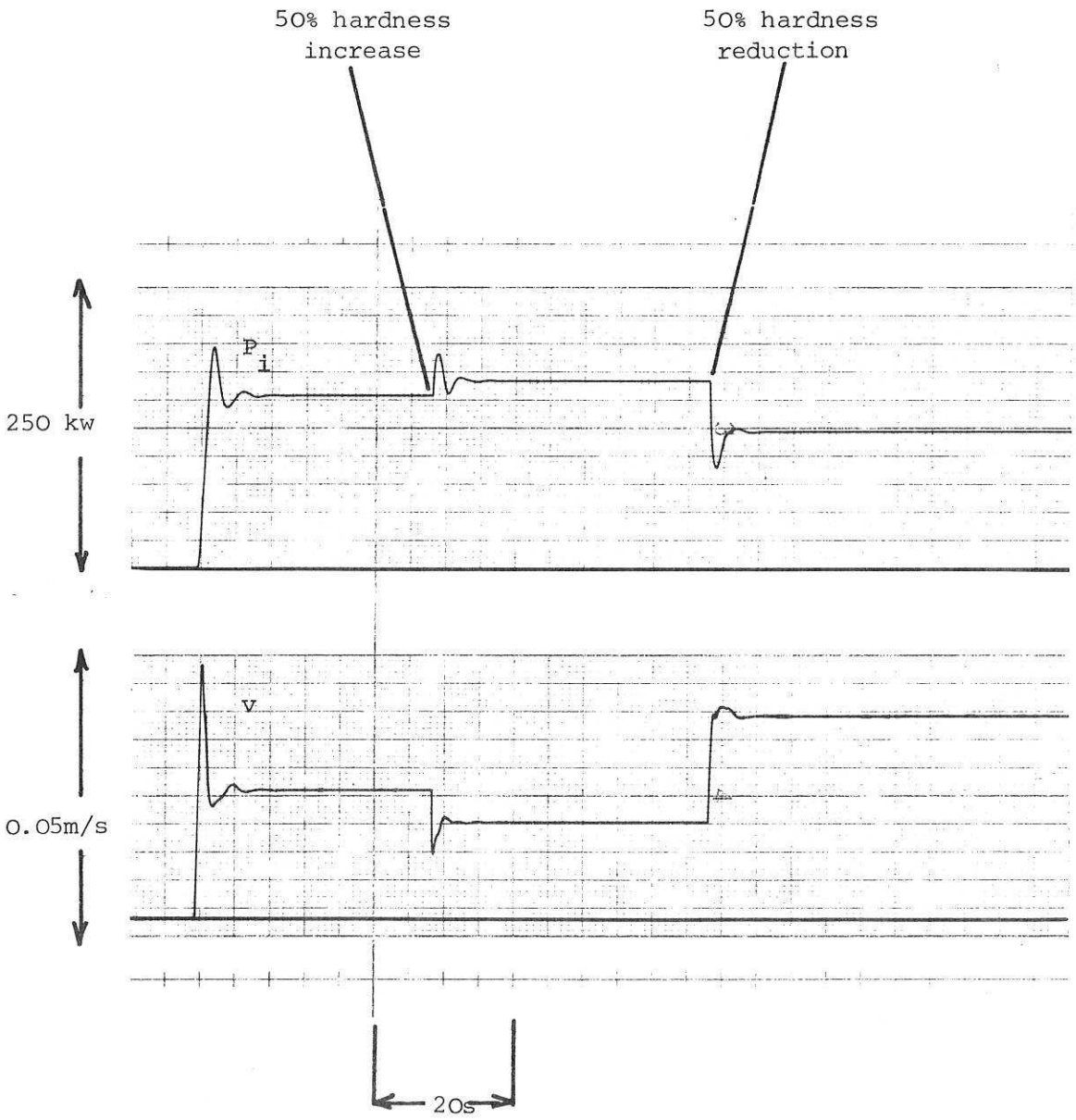

Fig. 13 N.C.B. controller in overriding mode with compensator added. Load gain setting = 50%, derivative gain setting = 70%.